The Mechanism of Anaphase Spindle Elongation: Uncoupling of Tubulin Incorporation and Microtubule Sliding during In Vitro Spindle Reactivation

Hirohisa Masuda, Kent L. McDonald, and W. Zacheus Cande

Department of Botany, University of California, Berkeley, California 94720

Abstract. To study tubulin polymerization and microtubule sliding during spindle elongation in vitro, we developed a method of uncoupling the two processes. When isolated diatom spindles were incubated with biotinylated tubulin (biot-tb) without ATP, biot-tb was incorporated into two regions flanking the zone of microtubule overlap, but the spindles did not elongate. After biot-tb was removed, spindle elongation was initiated by addition of ATP. The incorporated biot-tb was found in the midzone between the original half-spindles. The extent and rate of elongation were increased by preincubation in biot-tb. Serial section reconstruction of spindles elongating in tubulin and ATP showed that the average length of half-spindle microtubules increased due to growth of microtubules from the ends of native microtubules. The characteristic packing pattern between antiparallel microtubules was retained even in the "new" overlap region. Our results suggest that the forces required for spindle elongation are generated by enzymes in the overlap zone that mediate the sliding apart of antiparallel microtubules, and that tubulin polymerization does not contribute to force generation. Changes in the extent of microtubule overlap during spindle elongation were affected by tubulin and ATP concentration in the incubation medium. Spindles continued to elongate even after the overlap zone was composed entirely of newly polymerized microtubules, suggesting that the enzyme responsible for microtubule translocation either is bound to a matrix in the spindle midzone, or else can move on one microtubule toward the spindle midzone and push another microtubule of opposite polarity toward the pole.

THE mitotic spindle, a bipolar structure composed mainly of microtubules, is an apparatus for precisely distributing chromosomes to the two daughter cells. At anaphase, the two sets of chromatids are moved apart by two distinct processes on the spindle: chromosome-to-pole movement (anaphase A) and spindle elongation (anaphase B). Based on light and electron microscopy of spindles in vivo and biochemical studies of microtubules in vitro, several models have been proposed for the mechanism of spindle elongation. One model suggests that tubulin polymerization generates the force required for spindle elongation (Inoué and Sato, 1967; Brinkley and Cartwright, Jr., 1971; Pickett-Heaps et al., 1986). Addition of tubulin subunits to microtubules along their wall (Inoué and Sato, 1967) or to the minus ends of microtubules (the ends located at the spindle poles; Pickett-Heaps et al., 1986) would extend the microtubule length to push the spindle poles apart. A second model suggests that the force responsible for spindle elongation is produced by mechanochemical enzymes mediating the sliding apart of interdigitating sets of microtubules from the opposite half-spindles (McIntosh et al., 1969; McDonald et al., 1977, 1979; Margolis et al., 1978; Tippit et al., 1984; McIntosh et al., 1985; Saxton and McIntosh, 1987). In this model, tubulin polymerization would occur on the plus ends of microtubules, hence, on the ends located in the microtubule overlap zone (Margolis et al., 1978; Saxton and McIntosh, 1987), and be an auxiliary process that limits the rate or extent of spindle elongation (Nicklas, 1971). In addition to these models, some workers have proposed that forces generated outside the spindle pull the half-spindles apart (Aist and Berns, 1981; Heath, 1980; Kronebusch and Borisy, 1982).

When compared to more conventional spindles, diatom spindles have several unique features, which make them advantageous for studying spindle elongation. In the diatom, the apparatus responsible for spindle elongation, the central spindle, is comprised of two sets of microtubule bundles that interdigitate in the middle of spindle, whereas the components responsible for chromosome-to-pole movement are at the periphery (Pickett-Heaps and Tippit, 1978; McDonald et al., 1977, 1979). Since the interdigitated microtubules of the central spindle are fairly uniform in length, the zone of microtubule overlap is distinct and visible with phase-contrast

Dr. McDonald's present address is Department of Molecular, Cellular and Developmental Biology, University of Colorado, Boulder, Colorado 80309.

and polarized light microscopy (Pickett-Heaps et al., 1980; Cande and McDonald, 1985).

To study the mechanism of spindle elongation, we have developed an in vitro system in which spindles isolated from a diatom, *Stephanopyxis turris*, are capable of undergoing anaphase spindle elongation. With addition of ATP, the two half-spindles of the central spindle slide apart with a concomitant decrease in the zone of microtubule overlap (Cande and McDonald, 1985, 1986). When spindles were incubated in neurotubulin and ATP, they elongated several times more than the length of the overlap zone, and the extent and rate of elongation were dependent on tubulin concentration (Masuda and Cande, 1987). Using biotinylated tubulin (biot-tb)[1] to visualize the sites of tubulin incorporation, we found that new tubulin was first incorporated into two regions flanking the microtubule overlap zone. When elongation was more than the length of the overlap zone, biot-tb was then found as a single band in the spindle midzone. These results suggest that tubulin is incorporated onto the ends of microtubules in the overlap zone, and then slide through the midzone during spindle elongation.

To study the relationship of tubulin polymerization to microtubule sliding during spindle elongation in vitro, we developed a method of uncoupling these two processes. We show here that (*a*) tubulin polymerization does not generate the force for spindle elongation, whereas mechanochemical enzymes (the spindle motor) produces the force that slides the half-spindles apart; (*b*) tubulin polymerization increases the extent and rate of elongation; and (*c*) the tubulin polymerization, which contributes to spindle elongation, occurs onto the ends of microtubules in the overlap zone. For isolated spindles to behave in this fashion we deduce that the motor for microtubule sliding must remain stationary in the spindle midzone relative to the moving microtubules.

Materials and Methods

Preparation of Tubulin and Its Biotinylation

Beef brain tubulin was isolated from twice-cycled microtubule protein by ion exchange chromatography on DEAE-Sephadex, and biotinylated as described previously (Masuda and Cande, 1987). Unmodified tubulin and biot-tb were frozen in liquid nitrogen and stored in small aliquots at −80°C. A molecular mass of 110 kD was used for calculation of tubulin concentration.

Cell Culture and Synchronization

Stephanopyxis turris (stock no. L1272) was obtained from the Culture Collection of Marine Phytoplankton (Bigelow Laboratory for Ocean Services, West Boothbay, ME). Cells were grown in F/2 medium (Guillard, 1975) in suspension culture on a 6.5:17.5-h light/dark schedule at 18°C. 3 h before harvest, cells were drugged with 2×10^{-8} M nocodazole, and 20 min before harvest, cells were collected on 60-μm mesh Nitex filters and washed extensively to remove the drug (Cande and McDonald, 1986; Wordeman et al., 1986).

Spindle Isolation

Spindles were isolated as described by Masuda and Cande (1987) with a slight modification. 20 min after drug reversal, cells were harvested and rinsed with isotonic buffer (4.35 mM Tris, pH 8.0, 487 mM NaCl, 26.1 mM KCl, and 0.87 mM EGTA). Then, cells were suspended on ice in medium A (50 mM Pipes, pH 7.0, 10 mM $MgSO_4$, 10 mM EGTA, 40 mM sodium β-glycerophosphate, 1 mM dithiothreitol [DTT], 0.5 mM phenylmethylsulfonyl fluoride [PMSF], and proteolytic inhibitors [10 mg/liter soybean trypsin inhibitor, 10 mg/liter L-1-tosylamide-2-phenylethyl chloromethyl ketone, 10 mg/liter benzyl arginyl methyl ester, 10 mg/liter p-tosyl-L-arginine methyl ester, 1 mg/liter leupeptin, 1 mg/liter pepstatin A]) containing 50 μM ATPγS, 100 μM rac-6-hydroxy-2,5,7,8-tetramethyl-chromane-2-carboxylic acid (Trolox; Fluka Chemical Corp., Ronkonkoma, NY), 0.2% Brij 58, 1 μg/ml 4,6-diamidine-2-phenylindole dihydrochloride (DAPI), and 30% glycerol. The cells were homogenized on ice with a Kontes Dounce homogenizer, B pestle (Dounce, made by Kontes Glass Co., Vineland, NJ). The homogenate was filtered through 60-μm mesh and then 20-μm mesh Nitex filters. The filtrate from the homogenate was centrifuged onto coverslips through a 60% sucrose cushion containing medium A, 50 μM ATPγS, and 30 μM Trolox for 15 min at 4°C at 2,000 *g*. The coverslips were placed in medium A containing 30% glycerol, 50 μM ATPγS, and 30 μM Trolox and stored on ice until use.

Spindle Reactivation

After washed briefly in PMEG solution (75 mM Pipes, 2.5 mM $MgSO_4$, 5 mM EGTA, 40 mM sodium β-glycerophosphate, 1 mM DTT, and proteolytic inhibitors, pH 6.8) containing 20 μM taxol, and 30 μM Trolox, spindles on coverslips were reactivated at room temperature in PMEG solution containing 1 mM ATP, 0.1 mM GTP, 20 μM taxol, and 30 μM Trolox in the presence or absence of tubulin by putting 40 μl of the solutions directly onto coverslips. For the studies where tubulin polymerization was uncoupled from spindle elongation, spindles were washed in PMEG solution containing 0.1 mM ATPγS, 20 μM taxol, and 30 μM Trolox (solution B), and then incubated in 40 μl of biotinylated tubulin or unmodified tubulin and 0.1 mM GTP in solution B for 1–4 min at room temperature. The spindles were then washed in solution B for 30 s, and reactivated as described above. Spindle reactivation was terminated by placing the coverslip in PMEG solution containing 3.7% paraformaldehyde and 0.1% glutaraldehyde. After incubation in the solution for 15 min, coverslips were treated with 1 mg/ml sodium borohydride in PBS–methanol (1:1) solution for 5 min, 3 times in succession, and then processed for immunofluorescence microscopy. For electron microscopy, spindle reactivation was terminated by placing the coverslip in PMEG solution containing 1% glutaraldehyde.

Indirect Immunofluorescence

The mAbs against plant tubulin, specifically anti-mung bean tubulin (Mizuno et al., 1985) and anti-pear tubulin (Hogan, 1987), were kindly provided by Dr. Susan Wick and Dr. Brian Gunning, and Dr. Christopher Hogan, respectively. Biotinylated microtubules in spindles were visualized by incubation with rabbit anti-biotin (diluted to 1:100; Enzo Biochem Inc., New York, NY) for 30 min, and with fluorescein-conjugated sheep anti-rabbit IgG (1:80) for 30 min. Native microtubules of diatom spindles were visualized by incubation with mouse anti-plant tubulin (undiluted) for 1 h, followed by rhodamine-conjugated goat anti-mouse IgG (1:50) for 1 h. In some experiments, anti-plant tubulin was concentrated 4× using Centricon Microconcentrators (Amicon Corp., Danvers, MA) to obtain better staining. To visualize all microtubules in a spindle, the preparations were incubated with rabbit anti-sea urchin α-tubulin (1:100; Polysciences Inc., Warrington, PA) for 30 min and with sheep anti-rabbit IgG (1:80) for 30 min.

Measurement of Spindle and Overlap Zone Length, and Calculation of Extent of Tubulin Incorporation

Spindles were reactivated in unmodified tubulin and ATP for 0–4 min as described above. The spindle reactivation and tubulin incorporation were terminated by washing the spindles on coverslips in PMEG solution containing 20 μM taxol, 15 U/ml hexokinase, 5 mM glucose, and 30 μM Trolox. Then, the spindles were incubated in 40 μl of PMEG solution containing 5 μM biot-tb, 20 μM taxol, and 30 μM Trolox for 30 s. The spindles were fixed in formaldehyde and glutaraldehyde, reduced in sodium borohydride, and processed for immunofluorescence with anti-biotin and anti-plant tubulin, all as described above. Spindle and overlap zone lengths were measured from immunofluorescence images on a TV monitor using Zeiss Photoscope III and a DAGE-MTI low-light level TV camera. The average extent of tubulin polymerization onto the ends of the native microtubules in the overlap zone (see Fig. 10) was calculated using the average spindle length and the average overlap zone length as follows: extent of tubulin polymerization (T) = new half spindle length (NH) − original half spindle length (OH), where NH = (new spindle length + new overlap zone length)/2 and OH = (initial spindle length + initial overlap zone length)/2.

1. *Abbreviation used in this paper*: biot-tb, biotinylated tubulin.

Electron Microscopy and Serial Section Analysis

Spindles fixed in 1% glutaraldehyde in PMEG solution for 1 h were postfixed in 0.4% OsO_4 and 0.8% $K_3Fe(CN)_6$ in 0.1 M cacodylate buffer (pH 7.2), and then processed for electron microscopy and cross sectioned as described previously (Cande and McDonald, 1986). Sections were viewed and photographed at 20,000× magnification on a JEOL 100S electron microscope. Microtubules in the cross sections were tracked as described by McDonald et al. (1977).

Results

Uncoupling of Tubulin Polymerization from Spindle Elongation

We uncoupled tubulin polymerization from spindle elongation by relying on the different nucleotide requirements for each process. Previously we found that spindle elongation was specifically dependent on ATP, but tubulin was incorporated into spindles at room temperature in the absence of ATP (Masuda and Cande, 1987). Since spindles incubated at room temperature are functionally labile, we searched for conditions that preserved function. Addition of ATPγS (an ATP analogue) and Trolox (a radical scavenger) to the homogenization and incubation media increased retention of function during incubation at room temperature (Wordeman and Cande, 1987; Baskin and Cande, 1988).

Spindles were first incubated in 20 μM neuronal biot-tb and 20 μM taxol in the absence of ATP for 4 min. Biot-tb

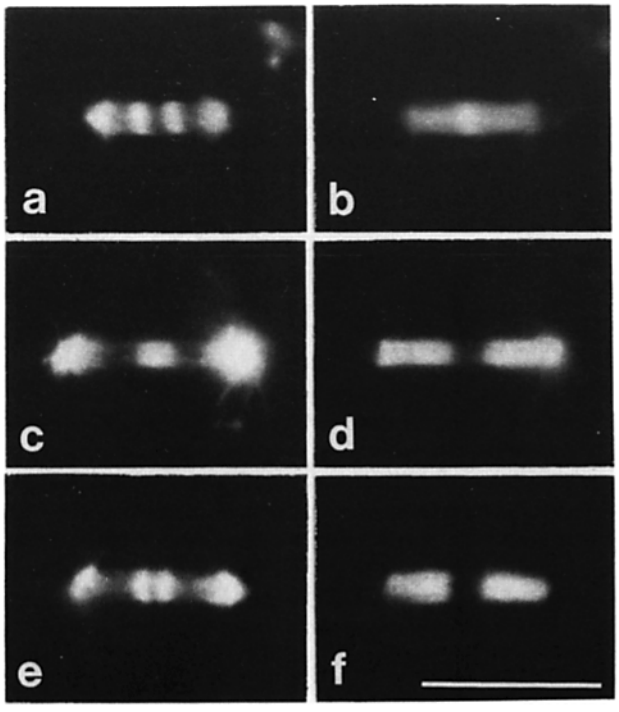

Figure 1. Immunofluorescence micrographs of spindles preincubated in neuronal tubulin and then reactivated in ATP. The spindles were double-stained with anti-biotin (*a*, *c*, and *e*) and with anti-plant tubulin (*b*, *d*, and *f*). Isolated spindles were first incubated in 20 μM biot-tb and 20 μM taxol for 4 min (*a* and *b*). After biot-tb was removed, the spindles were incubated in 1 mM ATP and 20 μM taxol for 1 min (*c* and *d*) or 2 min (*e* and *f*) at room temperature. Bar, 10 μm.

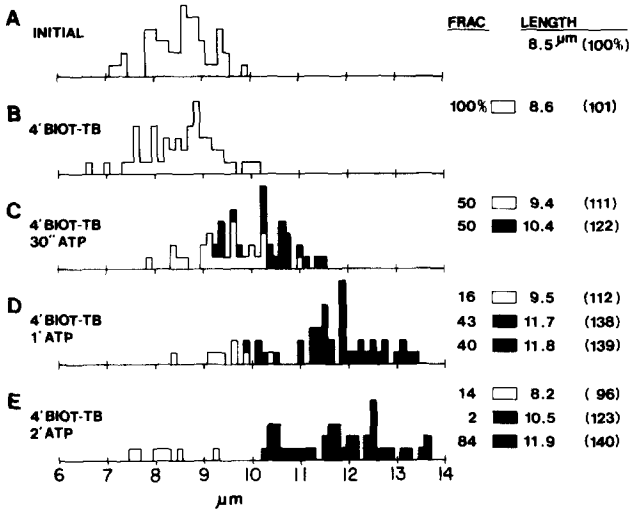

Figure 2. Length histograms of spindles preincubated in tubulin and then reactivated in ATP as shown in Fig. 1. (*A*) Without tubulin and ATP addition; (*B*) 4 min after addition of 20 μM biot-tb and 20 μM taxol; (*C*) 0.5 min, (*D*) 1 min, and (*E*) 2 min after addition of 1 mM ATP and 20 μM taxol. In *B–E*, spindles with immunofluorescence image, as shown in Fig. 1, *a* and *b*, *c* and *d*, and *e* and *f*, are indicated by □, ▩, and ■, respectively. Fraction (%) and average length (μm, or % of the initial spindle length) of spindles of each type are shown at the right side of the histogram.

was incorporated into two regions flanking the original overlap zone and around the poles (Fig. 1, *a* and *b*). Tubulin polymerization around the poles increased the apparent spindle length by 5–10% (data not shown). To measure spindle length without taking into account the astral-like tubulin incorporation around the poles, spindles were stained with anti-plant tubulin, which binds with high-affinity to diatom microtubules, but not well to neuronal tubulin (Mizuno et al., 1985; Hogan, 1987). The half-spindles did not move apart in biot-tb without ATP (Fig. 2, *A* and *B*). The length of the new overlap zone, which now includes the two regions of newly incorporated tubulin, was ~40% of the spindle length. After incubation for 4 min, free microtubules and dimers of biot-tb were removed by dilution, and the incorporated tubulin was stabilized by washing the spindles in a solution containing 20 μM taxol. When the spindles were then incubated in 1 mM ATP and 20 μM taxol, most of the spindles elongated to almost double the length of the original zone of microtubule overlap within 1 min (Fig. 1, *c* and *d*, and Fig. 2).

At 30 s after addition of ATP, we observed two types of spindles by immunofluorescence. Half of the spindles had a pattern of staining similar to the spindle shown in Fig. 1, *a* and *b*; that is, they showed two regions of incorporated biot-tb in the middle, and elongation was limited in that they had not formed a gap between the original half spindles (type I). The rest of the spindles had a pattern of staining similar to the spindle shown in Fig. 1, *c* and *d*; that is, they showed one broad band of incorporated biot-tb in the middle and had formed a gap between the original half spindles (type II). Type I and II spindles had an average length of 9.4 (111% of the original spindle length) and 10.4 μm (122%), respectively (Fig. 2 *C*). At 1 min after ATP addition, we observed

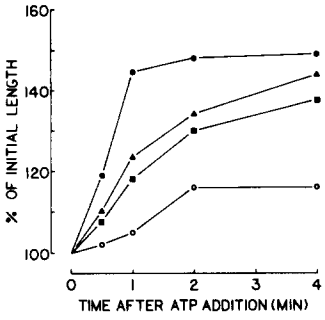

Figure 3. Dependence of the extent and rate of spindle elongation on tubulin concentration and preincubation time. Spindles were preincubated in 20 μM taxol and (●) 20 μM tubulin for 4 min, (▲) 5 μM tubulin for 4 min, or (■) 20 μM tubulin for 1 min. After tubulin was removed, the spindles were incubated in 1 mM ATP and 20 μM taxol. (○) Spindles without preincubation in tubulin were incubated in 1 mM ATP and 20 μM taxol. Lengths of more than 40 spindles were measured and averaged for each point.

three types of spindles. Type I spindles were decreased in number. Type II spindles were a similar percentage of the total spindle population as those at 30 s after ATP addition and had increased in average length to 11.7 μm (138%; Fig. 2 *D*). However, nearly one-half of the spindles had a new pattern of staining as shown in Fig. 1, *e* and *f* (type III). These showed two closely associated bands of incorporated biot-tb in the gap between the original half-spindles, and were 11.8 μm (139%) in length (Fig. 2 *D*). At 2 min after the addition, 80% of the spindles were type III and their average length was 11.9 μm (140%; Fig. 2 *E*).

Preincubation of spindles in tubulin increased not only the extent but also the rate of elongation (Fig. 3). These changes were dependent on the tubulin concentration, and on preincubation time, showing that the extent of tubulin incorporation affects the rate of elongation. Without preincubation in tubulin, spindles elongated at 0.8–1.0 μm/min, whereas with preincubation in 20 μM tubulin and 20 μM taxol for 4 min, the rate of elongation increased to 3.2–3.6 μm/min (*closed circle*, Fig. 3). This is one of the fastest rates we have observed in vitro, and is faster than the initial rate of elongation of spindles incubated in 20 μM tubulin, taxol, and ATP without any preincubation (1.2–1.6 μm/min; see Fig. 10; and Masuda and Cande, 1987).

Cross-sectional Structure of Elongating Spindle

To determine whether tubulin is polymerized onto the ends of native microtubules in the overlap zone, elongating spindles were cross sectioned for electron microscopy. Spindles were incubated for 1.5 min in the presence of 20 μM tubulin, 20 μM taxol, and 1 mM ATP, or in the absence of tubulin and ATP, and then duplicate samples were processed for electron microscopy and for immunofluorescence microscopy. Average spindle lengths determined by immunofluorescence with anti-plant tubulin were 8.0 ± 0.6 μm for the control spindles incubated in the absence of tubulin and ATP, and 11.0 ± 0.8 μm for the elongating spindles incubated in the presence of tubulin and ATP.

Fig. 4, *A* and *B* show microtubule numbers from cross sections for an elongating spindle and a control spindle, respectively. In the control spindle (Fig. 4 *B*), the microtubule number in the middle of the spindle (~700) was approximately twice the number in the other regions of the spindle (300–400). This microtubule distribution profile is

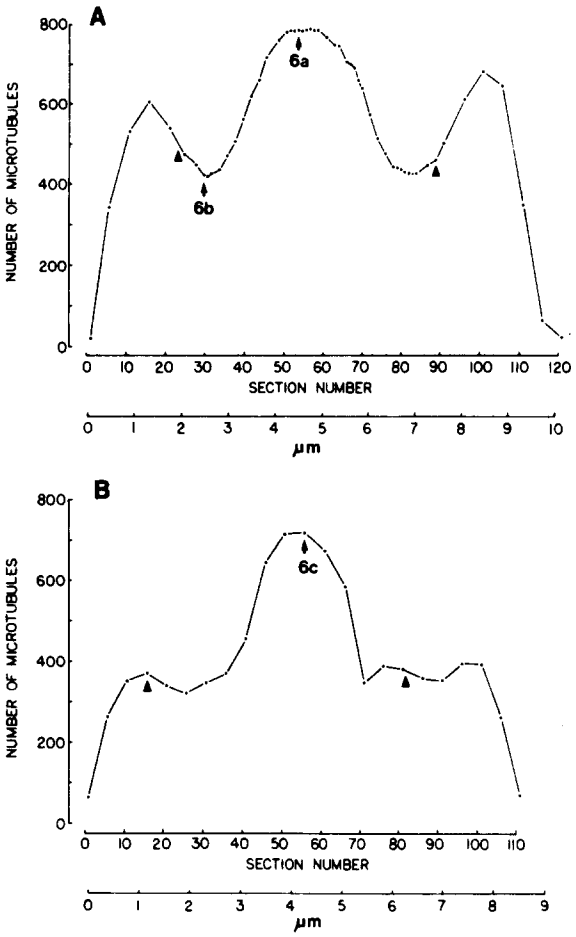

Figure 4. Microtubule distribution profiles of the elongating (*A*) and the control (*B*) spindles. (*A*) The spindle was incubated in 20 μM tubulin, 20 μM taxol, and 1 mM ATP for 1.5 min. (*B*) The spindle was incubated in 20 μM taxol in the absence of tubulin and ATP. The microtubules in the region between two arrowheads were partially reconstructed in Fig. 5. The regions labeled *6a*, *6b*, and *6c* indicate the positions of the sections used for Fig. 6, *a*, *b*, and *c*, respectively.

similar to that obtained from spindles of another diatom, *Diatoma vulgare*, which was shown to have an interdigitating set of microtubules in the spindle midzone (McDonald et al., 1977). The elongating spindle showed a similar microtubule distribution profile when compared to the control spindle except near the poles, where new microtubules nucleated from the pole complex increased the number of microtubules (Fig. 4 *A*). 600–700 microtubules were observed near the poles, and decreased to ~400 distal to the poles, and then increased to ~800 in the middle of the spindle. These results suggest that microtubules extending from both poles overlap in the middle of spindle both before and during spindle elongation, and that no extensive formation of free microtubules in the overlap zone has occurred.

To gather further evidence concerning the sites of tubulin incorporation and of anti-parallel microtubule interactions, microtubules in the spindles were partially reconstructed in the regions including the overlap zone (Fig. 5, *A* and *B*). For the spindle elongating in tubulin, most microtubules had only one free end in the reconstructed region. For 340 tracked

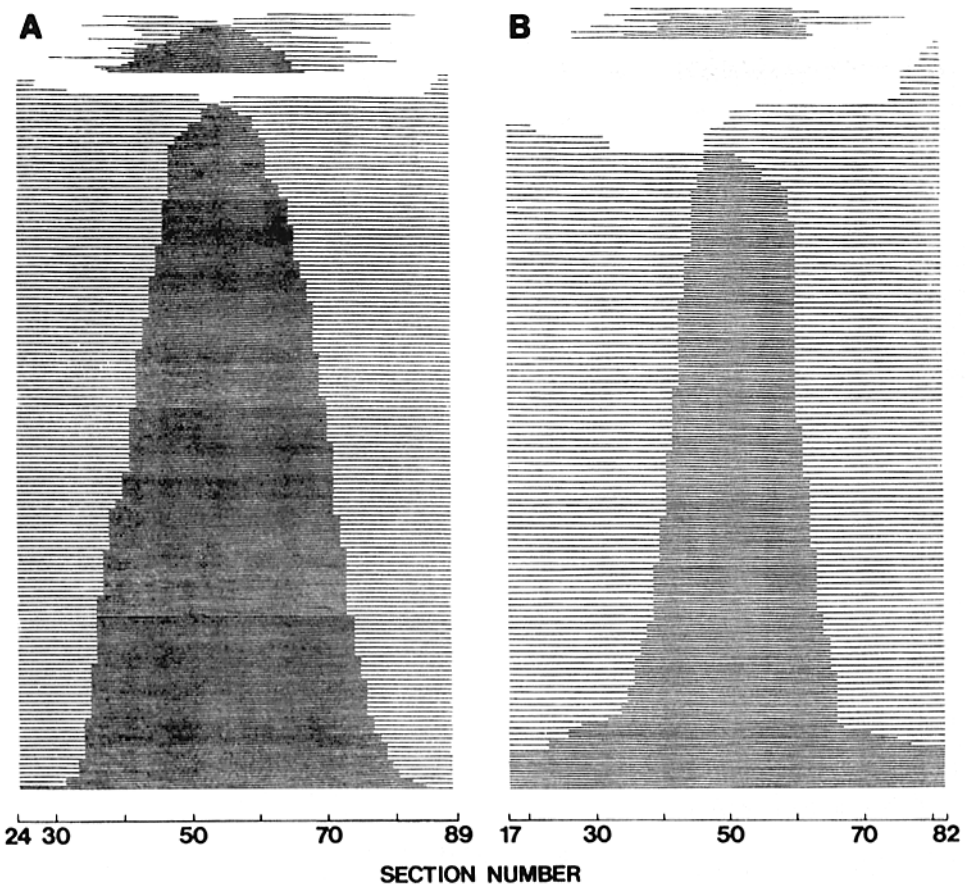

Figure 5. The distribution of individual microtubules from the elongating (*A*) and the control (*B*) spindles. Microtubules in several bundles of the elongating or control spindle were tracked through the 66 serial sections in the region between the arrowheads in Fig. 4. Each line represents a single microtubule.

microtubules, we found 157 microtubules with one free right end, 157 with one free left end, 25 microtubule fragments that had both ends free, and one continuous microtubule in the reconstructed region. Most microtubules with one free end overlapped other microtubules of opposite polarity in the middle of the spindle. A similar result was obtained from the reconstruction of microtubule distribution in the control spindle. For 255 tracked microtubules, we found 108 microtubules with a free right end, 122 with a free left end, 11 microtubule fragments, and 14 continuous microtubules. As above, most of the microtubules with opposite polarities overlapped in the middle of spindle.

Measurement of the phase-contrast image of the embedded spindle before sectioning shows that the elongating spindle was 10.1 μm in length. If we assume that the length of the original overlap zone is 25% of the initial spindle length (Cande and McDonald, 1986), microtubules of the initial half-spindle were calculated to be 5.0 ± 0.4 μm in length. Microtubules of each half-spindle were 6.3 μm in average length and so were ~0.9–1.7 μm longer than microtubules of the initial half-spindle. Immunofluorescence microscopy of elongating spindles double-stained with anti-plant tubulin and with anti-sea urchin α-tubulin, which stains both diatom spindles and neuronal tubulin, showed that the increase in overall spindle length was very similar to the increase in pole-to-pole distance of the original half-spindles, even though we had usually overestimated the average spindle length increase because of tubulin incorporation around the poles (data not shown). These results show that tubulin is polymerized onto the ends of native microtubules in the overlap zone during elongation.

Microtubule packing and the spatial relationships of antiparallel microtubules can be observed in spindle cross sections. Selected sections from the spindle in Fig. 4 are shown in Figs. 6 and 7 and are accompanied by diagrams of microtubule polarity. In the middle of the elongating spindle (Fig. 6, *a* and *a'*), microtubules extending from both poles overlapped to form closely packed bundles, similar to the bundles found in the middle of the control spindle (Fig. 6, *c* and *c'*). The packing pattern of microtubules in the bundles usually was hexagonal but sometimes square (see Fig. 7). As one starts from the middle of the overlap zone and proceeds toward one pole, microtubules from the other pole decreased, almost disappearing by about the position of the sections in Fig. 6, *b* and *b'*, and then new short microtubules from the same pole started to appear and increased in number in the sections closer to that pole. No closely packed microtubule bundles were observed in regions other than in the overlap zone. We found many cross-bridges connecting antiparallel or parallel microtubules in the overlap zone of the elongating (Fig. 7) and control (data not shown) spindles. To estimate the extent of antiparallel interaction, we determined the polarity of neighboring microtubules. The number of parallel and antiparallel microtubules found within a circle 45 nm in radius centered on a given microtubule were scored. For 55 microtubules analyzed (*closed circle*, Fig. 7) antiparallel neighbors were almost 2.5 times more frequent than parallel ones.

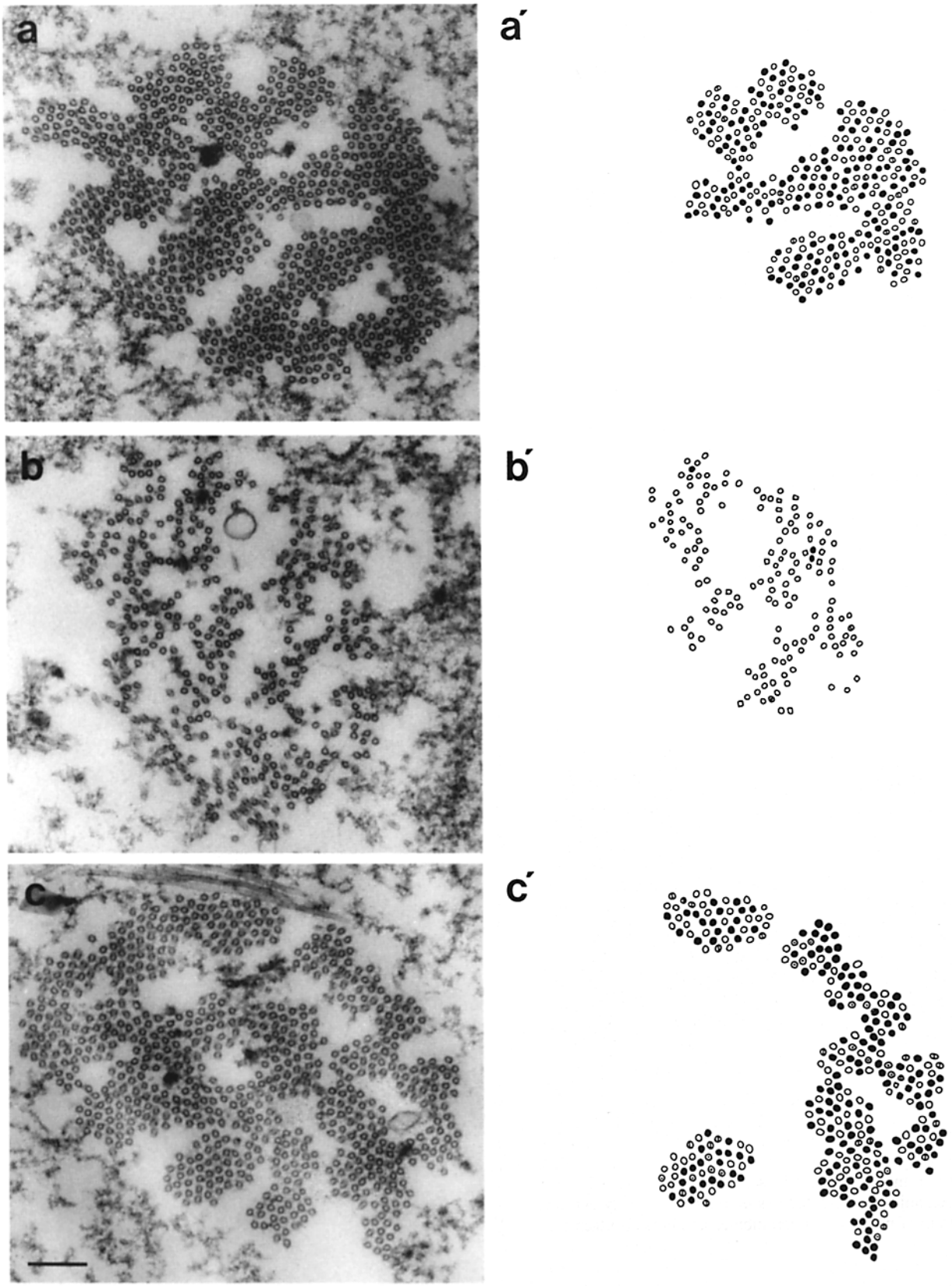

Figure 6. (*a–c*) Electron micrographs of cross sections from the elongating and the control spindles. The positions of the sections in the spindles are indicated in Fig. 4. (*a'–c'*) Diagrams of polarity of microtubules in the sections *a–c*. (○) Microtubules of one free right end in the reconstructed regions in Fig. 5; (●) microtubules of one free left end; (⊕) microtubule fragments with two free ends; and (⊙) continuous microtubules. Bar, 0.2 μm.

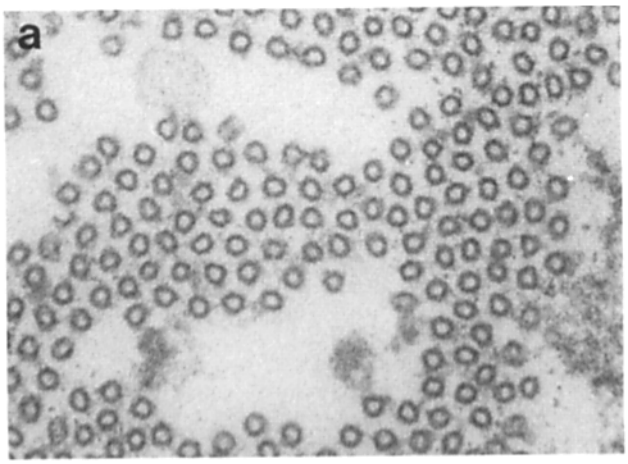

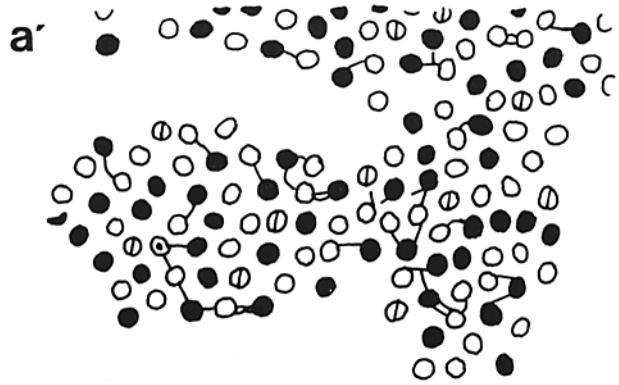

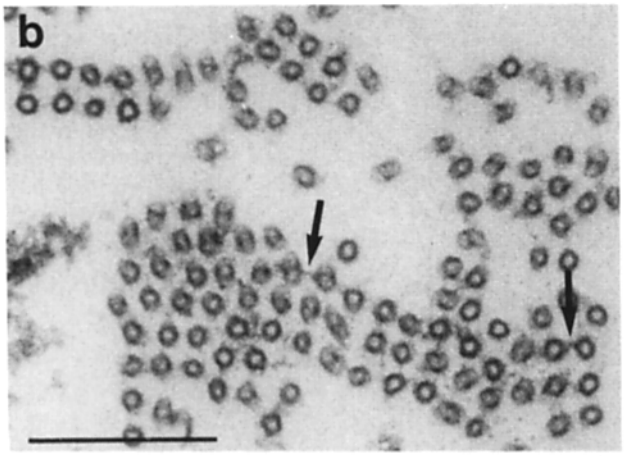

Figure 7. (*a* and *b*) Electron micrographs at higher magnification of cross sections through the overlap zone of elongating spindles. (*a*) A section from the spindle in Figs. 4 *A* and 5 *A*; (*b*) a section from other elongating spindle in the same preparation as *a*. Note the tendency for microtubules to be square-packed arrays. Connections between adjacent microtubules (*arrows*) are clearly evident. (*a'*) A diagram of polarity of microtubules and cross-bridges connecting microtubules in the section *a*. Cross-bridges connecting microtubules or arms projecting from microtubules are shown as lines. ○, ●, ⊙, and ⊙ indicate the polarity of microtubules as shown in the legend of Fig. 6, *a'–c'*. Bar, 0.2 μm.

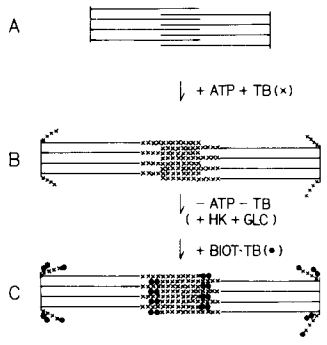

Figure 8. Scheme for determination by immunofluorescence of the site of microtubule overlap during spindle elongation. Isolated spindles (*A*) were incubated in 20 μM taxol, and various concentrations of tubulin and ATP for 0–2 min (*B*). Tubulin and ATP were removed by washing in a solution containing hexokinase, glucose, and taxol to terminate spindle elongation and tubulin incorporation. The spindles were then incubated in 5 μM biot-tb and 20 μM taxol for 30 s to label the microtubule ends (*C*). The labeled microtubule ends and the original half spindles were visualized by staining with anti-biotin and anti-plant tubulin, respectively.

Site of Microtubule Overlap and Extent of Tubulin Incorporation Determined by Immunofluorescence

We measured the length of the zone of microtubule overlap during spindle elongation and its position relative to the original half spindles, using the method illustrated in Fig. 8. Spindles were incubated in unmodified neuronal tubulin, taxol, and ATP for 0–2 min. Spindle elongation and tubulin incorporation was terminated by washing the spindles with a solution containing hexokinase, glucose, and taxol. This medium blocked further spindle elongation by removing all ATP (Masuda and Cande, 1987). Spindles were then incubated in 5 μM biot-tb for 30 s to label microtubule ends with biot-tb. After fixation, spindles were double-labeled with anti-biotin and anti-plant tubulin for immunofluorescence.

In spindles without preincubation in tubulin and ATP, biot-tb was incorporated into the two regions flanking the overlap zone and around the poles (Fig. 9 *A*, *a* and *b*). The center-to-center distance between the two regions of incorporated biot-tb was ~25% of the total spindle length on average in this preparation. This is similar to direct measurements of overlap zone sizes made with polarization optics (Cande and McDonald, 1985). Fig. 9 *A*, *c–h* shows immunofluorescence micrographs of elongating spindles in 20 μM tubulin, 20 μM taxol, and 1 mM ATP. At 30 s after addition of tubulin and ATP, the length of the overlap zone had increased (Fig. 9 *A*, *c* and *d*). With further spindle elongation, the overlap zone length then decreased, and a gap appeared between the two original half-spindles. At 1.5 min after ATP addition, the overlap zone length of many spindles was similar to the size of a gap between the original half-spindles (Fig. 9 *A*, *e* and *f*). At 2 min, the spindles had elongated further and the overlap zone length of many spindles was shorter than the size of the gap between the original half-spindles, showing that overlap zone is composed entirely of new microtubules (Fig. 9 *A*, *g* and *h*). The zone of biot-tb incorporation increased during spindle elongation, which is consistent with results from electron microscopy that showed a broadening of the distribution of the microtubule ends of the elongating spindle as compared to the control spindle (Fig. 5). These results are interpreted in a diagram (Fig. 9 *B*). Our results show that spindles continued to elongate even after the overlap zone is composed entirely of newly polymerized microtubules.

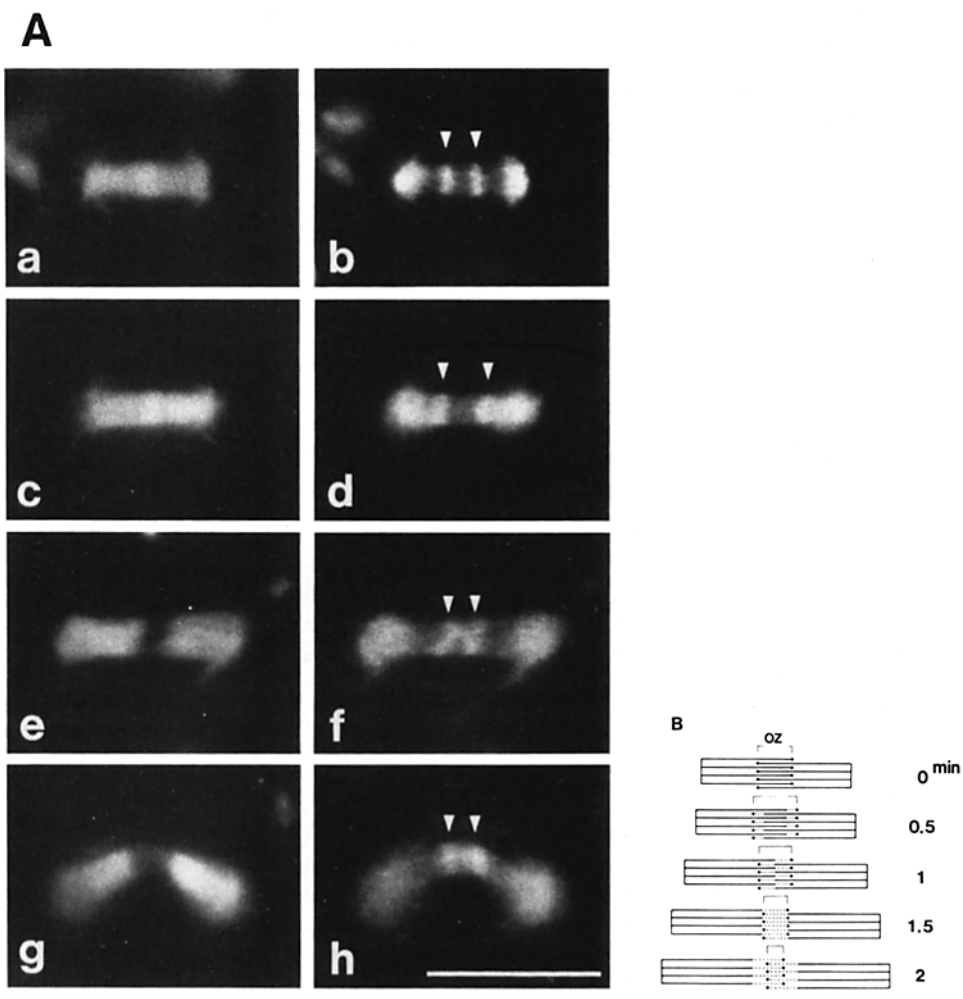

Figure 9. (*A*) Visualization of the sites of microtubule overlap during spindle elongation relative to the sites of the original half-spindles by immunofluorescence. Spindles were incubated in 20 μM taxol, 20 μM tubulin, and 1 mM ATP for 0–2 min, and then processed as described in Fig. 8. (*a*, *c*, *e*, and *g*) Spindles stained with anti-plant tubulin; (*b*, *d*, *f*, and *h*) spindles stained with anti-biotin. *a* and *b*, spindle before addition of tubulin and ATP; *c* and *d*, 30 s after the addition; *e* and *f*, 1.5 min after; *g* and *h*, 2 min after. Arrowheads in *b*, *d*, *f*, and *h* indicate the sites of the microtubule ends of the overlap zone. (*B*) Diagram of spindle elongation in the presence of 20 μM tubulin, 20 μM taxol, and 1 mM ATP. This shows averaged images of spindles based on the data from Fig. 10. Newly polymerized microtubules onto the native microtubules in the overlap zone are shown as (- - - -). Microtubule ends labeled by biotb are shown as (●). *OZ*, zone of microtubule overlap. Bar, 10 μm.

These results suggest that the spindle motor, which produces the sliding between antiparallel microtubules in the overlap zone, remains in the middle of the spindle during elongation and interacts with newly polymerized microtubules.

Spindle and overlap zone length and tubulin incorporation were dependent on tubulin and ATP concentrations (Fig. 10). Spindles elongated more slowly in 0.1 mM ATP than in 1.0 mM ATP. The overlap zone remained broad in 0.1 mM ATP, whereas in 1.0 mM ATP it narrowed with elongation. The extent of tubulin incorporation onto the ends of microtubules in the overlap zone in 0.1 mM ATP was similar to that in 1.0 mM ATP, but was greater than in the absence of ATP. In higher concentrations of tubulin, spindles elongated faster, tubulin polymerization was greater, and the overlap zone length was longer for the same time points. There was no obvious relationship between the rate of elongation and the rate of tubulin incorporation.

To determine how ATP increases the extent of tubulin polymerization onto the ends of microtubules in the overlap zone, we examined the effects of other nucleotides and vanadate on this process. Although vanadate blocked spindle elongation (Masuda and Cande, 1987), it did not block the

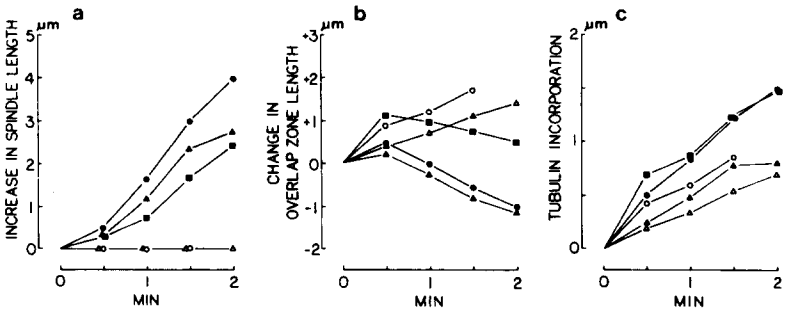

Figure 10. Effects of ATP and tubulin on spindle length (*a*), overlap zone length (*b*), and extent of tubulin incorporation (*c*). Spindles were incubated in 20 μM taxol and (●) 20 μM tubulin and 1 mM ATP, (▲) 5 μM tubulin and 1 mM ATP, (■) 20 μM tubulin and 0.1 mM ATP, (○) 20 μM tubulin and no ATP, or (△) 5 μM tubulin and no ATP. They were then processed for determination of the sites of the microtubule overlap as described in Fig. 8. Extent of tubulin incorporation was calculated using the spindle length and the overlap zone length as described in Materials and Methods. n = 40–120 spindles per point on graph.

increased incorporation of tubulin onto the end of microtubules in the overlap zone. ADP (1 mM) stimulated tubulin incorporation onto microtubule ends, but ITP, ATPγS, and GTP (1 mM) did not (data not shown). These results indicate that spindle elongation is not required for an increase in tubulin incorporation onto the end of microtubules in the overlap zone.

Discussion

Mechanism of Force Generation and Role of Tubulin Polymerization

Previously we have shown that spindle elongation both in the presence and absence of tubulin requires ATP and is inhibited by vanadate or AMPPNP (Masuda and Cande, 1987). This suggests that spindles elongate in the presence of tubulin by the same ATP-dependent mechanism as in its absence. Since tubulin incorporation into isolated spindles does not require ATP (Masuda and Cande, 1987), it was possible to uncouple tubulin incorporation from spindle elongation. With no ATP, biot-tb was incorporated into two regions flanking the microtubule overlap zone and around the poles (Type I; Fig. 1, *a* and *b*). Spindle elongation could be initiated by addition of ATP after free tubulin was removed. This resulted in changes in the pattern of incorporated biot-tb and gap formation between the original half-spindles (Type II; Fig. 1, *c* and *d*). The final extent of spindle elongation was similar to the length of the new overlap zone; i.e., the equivalent of the original overlap zone plus the two incorporated regions of biot-tb. The formation of a gap between the new half-spindles after elongation is complete (Type III; Fig. 1, *e* and *f*) is due to depolymerization of the biotinylated microtubules from the plus ends polewards. These results eliminate models, which suggest that tubulin incorporation along the microtubule wall (Inoue and Sato, 1967) or onto the minus ends of microtubules (Pickett-Heaps et al., 1986) produces the forces needed for spindle elongation. There is no free tubulin available during the spindle elongation induced by ATP. As shown by monitoring spindles on-line with polarization optics, the size of the half-spindle remains constant during spindle elongation (T. Baskin and W. Z. Cande, unpublished observations). After spindle elongation has been completed, the original half-spindles are separated by a large gap filled with biotinylated microtubules (Figs. 1 and 2). These results are also consistent with the changes in patterns of tubulin incorporation seen when spindles are elongating in the presence of tubulin (Masuda and Cande, 1987). Before spindles have elongated by the equivalent of the overlap zone, there are two regions of incorporated tubulin flanking the overlap zone. After further elongation, there is one broad zone of incorporated tubulin in the spindle midzone (Masuda and Cande, 1987). Electron microscopy of cross-sectioned spindles showed that there were few microtubule fragments in the spindles elongating in tubulin and ATP (Fig. 5), suggesting that the diatom microtubules in each half-spindle were extended during spindle elongation. Taking these results together, we conclude that the force required for in vitro spindle elongation is produced by the mechanochemical enzymes that push apart antiparallel microtubules from the opposite half-spindles. Tubulin is polymerized onto the ends of microtubules in the overlap zone and its role during spindle elongation is to increase the extent of sliding.

Our in vitro results are consistent with in vivo results recently described by Saxton and McIntosh (1987). Using microinjection of fluorescein-labeled tubulin and laser microbeam photobleaching, they found that labeled tubulin adds onto the plus ends of interdigitated microtubules in late anaphase and telophase spindles of PtKl cells, and that the two half-spindles move apart as discrete units.

Several investigators have suggested that forces generated outside the spindle pull the spindle poles apart (Aist and Berns, 1981; Heath, 1980; Kronebusch and Borisy, 1982). However, Saxton and McIntosh (1987) have shown in late anaphase-telophase of PtKl cells that some antiparallel sliding occurs after the poles have detached from the interzone microtubules. Leslie and Pickett-Heaps (1983), using microbeam irradiation of the central spindle in the diatom *Hantzschia*, have demonstrated that the force for spindle elongation is apparently generated in the zone of microtubule overlap. For isolated diatom spindles, we have shown that there are no cytoplasmic structures attached to the poles to pull them apart (Cande and McDonald, 1985; McDonald et al., 1986). Therefore, the sliding apart of the interdigitated microtubules of each half-spindle due to mechanochemical interactions between them must contribute significantly to spindle elongation in many types of cells. However, this does not eliminate the possibility that external forces applied to the spindle poles may also contribute to anaphase B in some spindles.

The rate of spindle elongation was increased by preincubation in tubulin, and was dependent on tubulin concentration and on preincubation time (Fig. 3). We have previously observed that when spindles were reactivated in tubulin and ATP, the rate of elongation was dependent on tubulin concentration (Masuda and Cande, 1987). The rate of anaphase spindle elongation in vivo was 1.7 μm/min on average (range 1.4–3.2 μm/min; McDonald et al., 1986). The in vivo rate was less than the maximal rate of elongation we have observed in vitro with spindles preincubated in tubulin (~3.6 μm/min), but was greater than the rate of elongation of spindles without preincubation in tubulin (0.8–1.0 μm/min). These results suggest that the concentration of polymerization-competent tubulin at the ends of microtubules in the overlap zone may determine or limit the rate of elongation during anaphase B in vivo. Tubulin polymerization may increase the ATPase activity and/or the number of motors involved in the sliding of half-spindles; although, at present, we do not have any data to evaluate these possibilities.

In some cells, including *S. turris*, the size of the zone of microtubule overlap does not seem to change during anaphase spindle elongation in vivo (Tippit et al., 1980; McDonald et al., 1986). In other cells, the overlap zone length decreases with spindle elongation (McDonald et al., 1977; Pickett-Heaps et al., 1980; Tippit et al., 1984; McIntosh et al., 1985). It was possible to manipulate the overlap zone length in vitro by changing the ATP and tubulin concentrations (Fig. 10). We do not know how spindle elongation is initiated at anaphase, but microtubule sliding and tubulin polymerization onto the ends of the interdigitated microtubules must be activated. After it is initiated, it may be regulated by the ATP concentration and/or the concentration of poly-

merization-competent tubulin dimer. This suggests that differences in overlap zone behavior in various cell types during anaphase B may be due to differencs in coordination of microtubule sliding and tubulin polymerization rate rather than any fundamental changes in spindle mechanochemistry.

The rate of tubulin incorporation onto the ends of microtubules in the overlap zone was increased in the presence of ATP (Fig. 10). This increase is not dependent on spindle elongation, since it occurred even in the presence of ATP and vanadate, which inhibits spindle elongation, and since ADP is also effective in increasing the rate of tubulin incorporation (data not shown). The effect of ATP and ADP on the extent of tubulin incorporation may be due to an enhancement of tubulin polymerization specific for the microtubule ends in the overlap zone. However, there are other possible interpretations consistent with our observations.

The Nature of the Spindle Motor

The motor responsible for the movement apart of the half-spindles must be located in the region of the spindle that includes the zone of microtubule overlap. In the overlap zone, microtubules were not distributed at random, but preferred antiparallel near neighbors, as shown by McDonald et al. (1979). We have also observed cross-bridges connecting antiparallel microtubules (Fig. 7). However, the spindle motor must also interact with newly polymerized microtubules without remaining permanently attached to the old microtubules, since spindles can elongate after the overlap zone is made entirely of new microtubules. In one possible model, we would imagine that the motor would translocate on one microtubule toward the spindle midzone, while it pushes another microtubule toward the opposite pole. Alternatively, the motor may not directly cross-link antiparallel microtubules but would be bound to another structural component, a matrix, in the spindle midzone. A visible manifestation of this matrix may be the osmiophilic fuzz seen as an intermicrotubule matrix in the midzone of many different spindles (cf. McDonald et al., 1977).

Wordeman and Cande (1987) have recently shown that reactivation of diatom spindle elongation is correlated with the phosphorylation of a 205-kD spindle-associated protein. The 205-kD protein can be thiophosphorylated when spindles are preincubated in ATPγS. As demonstrated using an antibody against thiophosphoproteins, this protein is located predominantly in the zone of microtubule overlap. During spindle elongation in ATP in the absence of tubulin, the staining of the midzone decreases in width and intensifies in brightness, in parallel with a decrease in the zone of microtubule overlap. In spindles that have been preincubated in biot-tb and ATPγS, the midzone label does not move out onto the biot-tb but remains centrally located in a broad band and eventually colocalizes with the biotinylated microtubules when they move from the periphery into the spindle midzone during reactivation (Wordeman, Masuda, and Cande, manuscript submitted for publication). These results suggest that the distribution of the 205-kD protein is determined by the overlap zone and that this protein and perhaps other proteins in the overlap zone remain stationary even as microtubules slide through it. As described in vivo, McDonald et al. (1977) have shown that in *Diatoma vulgare*, an intermicrotubule matrix in the microtubule overlap zone increases in its staining density as the length of the overlap zone decreases. We postulate that the 205-kD protein and the spindle motor may be a component of this intermicrotubule matrix. Further studies of the 205-kD protein and associated proteins will clarify the nature of spindle motor and the role of the midzone matrix during spindle elongation.

We thank Tobias Baskin, Chris Staiger, and Linda Wordeman for helpful discussions; Chris Hogan, Susan Wick, and Brian Gunning for gifts of antibodies; and Doug Ohm and Barbara Brady for technical assistance. We thank Dr. Matthew Suffness, National Products Branch, Division of Cancer Treatment, National Cancer Institute, Bethesda, Maryland for a gift of taxol.

This work was supported by National Institutes of Health grant GM-23238 to W. Z. Cande and a senior fellowship from the Muscular Dystrophy Association to H. Masuda. W. Z. Cande has an appointment as a Research Professor in the Miller Institute for Basic Research Science.

Received for publication 11 February 1988, and in revised form 18 April 1988.

References

Aist, J. R., and M. W. Berns. 1981. Mechanics of chromosome separation during motosis in *Fusarium (Fungi imperfecti)*: new evidence from ultrastructural and laser microbeam experiments. *J. Cell Biol.* 91:446–458.

Baskin, T., and W. Z. Cande. 1988. Direct observation of mitotic spindle elongation in vitro. *Cell Motil. Cytoskeleton.* In press.

Brinkley, B. R., and J. Cartwright, Jr. 1971. Ultrastructural analysis of mitotic spindle elongation in mammalian cells in vitro. *J. Cell Biol.* 50:416–431.

Cande, W. Z., and K. L. McDonald. 1985. *In vitro* reactivation of anaphase spindle elongation using isolated diatom spindles. *Nature (Lond.).* 316: 168–170.

Cande, W. Z., and K. L. McDonald. 1986. Physiological and ultrastructural analysis of elongating mitotic spindles reactivated in vitro. *J. Cell Biol.* 103: 593–604.

Guillard, R. R. L. 1975. Culture of phytoplankton for feeding marine invertebrates. *In* Culture of Marine Invertebrate Animals. W. L. Smith and M. H. Chanley, editors. Plenum Publishing Corp., New York. 29–60.

Heath, B. 1980. Variant mitoses in lower eukaryotes: indicators of the evolution of mitosis? *Int. Rev. Cytol.* 64:1–80.

Hogan, C. J. 1987. Microtubule patterns during meiosis in two higher plant species. *Protoplasma.* 138:126–136.

Inoué, S., and H. Sato. 1967. Cell motility by labile association of molecules: the nature of mitotic spindle fibers and their role in chromosome movement. *J. Gen. Physiol.* 50:259–292.

Kronebusch, P. J., and G. G. Borisy. 1982. Mechanics of anaphase B movement. *In* Biological Functions of Microtubules and Related Structures. H. Sakai, H. Mohri, and G. G. Borisy, editors. Academic Press, Inc., New York. 233–245.

Leslie, R. J., and J. D. Pickett-Heaps. 1983. Ultraviolet microbeam irradiations of mitotic diatoms: investigation of spindle elongation. *J. Cell Biol.* 96:548–561.

Margolis, R. L., L. Wilson, and B. I. Kiefer. 1978. Mitotic mechanism based on intrinsic microtubule behavior. *Nature (Lond.).* 272:450–452.

Masuda, H., and W. Z. Cande. 1987. The role of tubulin polymerization during spindle elongation in vitro. *Cell.* 49:193–202.

McDonald, K. L., M. K. Edwards, and J. R. McIntosh. 1979. Cross-sectional structure of the central mitotic spindle of *Diatoma vulgare*. Evidence for specific interactions between antiparallel microtubules. *J. Cell Biol.* 83:443–461.

McDonald, K. L., K. Pfister, H. Masuda, L. Wordeman, C. Staiger, and W. Z. Cande. 1986. Comparison of spindle elongation *in vivo* and *in vitro* in *Stephanopyxis turris*. *J. Cell Sci.* 5(Suppl.):205–227.

McDonald, K., J. D. Pickett-Heaps, J. R. McIntosh, and D. H. Tippit. 1977. On the mechanism of anaphase spindle elongation in *Diatoma vulgare*. *J. Cell Biol.* 74:377–388.

McIntosh, J. R., P. K. Helper, and D. G. van Wie. 1969. Model for mitosis. *Nature (Lond.).* 224:659–663.

McIntosh, J. R., U.-P. Roos, B. Neighbors, and K. L. McDonald. 1985. Architecture of the microtubule component of mitotic spindles from *Dictyostelium discoideum*. *J. Cell Sci.* 75:93–129.

Mizuno, K., F. Sek, J. Perkin, S. Wick, J. Duniec, and B. Gunning. 1985. Monoclonal antibodies specific to plant tubulin. *Protoplasma.* 129:100–108.

Nicklas, R B. 1971. Mitosis. *In* Advances in Cell Biology. D. M. Prescott, L. Goldstein, and E. McConkey, editors. Appleton-Century-Croft, New York. 225–297.

Pickett-Heaps, J. D., and D. H. Tippit. 1978. The diatom spindle in perspective. *Cell.* 14:455–467.

Pickett-Heaps, J. D., D. H. Tippit, S. A. Cohn, and T. P. Spurck. 1986. Microtubule dynamics in the spindle. Theoretical aspects of assembly/disassembly reactions *in vivo*. *J. Theor. Biol.* 118:153–169.

Pickett-Heaps, J. D., D. H. Tippit, and R. Leslie. 1980. Light and electron microscopic observations on cell division in two large pennate diatoms, *Hantzschia* and *Nitzschia*. I. Mitosis *in vivo*. *Eur. J. Cell Biol.* 21:1–11.

Saxton, W. M., and J. R. McIntosh. 1987. Interzone microtubule behavior in late anaphase and telophase spindles. *J. Cell Biol.* 105:875–886.

Tippit, D. H., C. T. Fields, K. L. O'Donnell, J. D. Pickett-Heaps, and D. J. McLaughlin. 1984. The organization of microtubules during anaphase and telophase spindle elongation in the rust fungus *Puccina*. *Eur. J. Cell Biol.* 34:34–44.

Tippit, D. H., L. Pillus, and J. D. Pickett-Heaps. 1980. Organization of spindle microtubules in *Ochromonas danica*. *J. Cell Biol.* 87:531–545.

Wordeman, L., and W. Z. Cande. 1987. Reactivation of spindle elongation *in vitro* is correlated with the phosphorylation of a 205 kd spindle-associated protein. *Cell.* 50:535–543.

Wordeman, L., K. L. McDonald, and W. Z. Cande. 1986. The distribution of cytoplasmic microtubules throughout the cell cycle of the centric diatom *Stephanopyxis turris*: their role in nuclear migration and positioning the mitotic spindle during cytokinesis. *J. Cell Biol.* 102:1688–1698.